Article

Developmental Cell

POS-1 Promotes Endo-mesoderm Development by Inhibiting the Cytoplasmic Polyadenylation of *neg-1* mRNA

Highlights

- Endo-mesoderm fate is a product of both SKN-1 presence and NEG-1 absence
- POS-1 represses expression of *neg-1* by preventing cytoplasmic polyadenylation
- Transcriptome-wide quantification shows that poly(A) tail length changes in *C. elegans*
- GLD-3/Bicaudal-C function is conserved in embryonic fate specification

Authors

Ahmed Elewa, Masaki Shirayama, Ebru Kaymak, ..., Traude H. Beilharz, Sean P. Ryder, Craig C. Mello

Correspondence

craig.mello@umassmed.edu

In Brief

The RNA-binding protein POS-1 promotes endo-mesoderm development in *C. elegans* embryos. Elewa et al. show that POS-1 functions by opposing the cytoplasmic polyadenylation of the gut antagonist *neg-1*, therefore preventing *neg-1* accumulation and allowing endo-mesoderm development. Transcriptome-wide studies suggest a similar regulation of other embryonic transcripts.

Accession Numbers

GSE57993

Elewa et al., 2015, Developmental Cell *34*, 1–11
July 6, 2015
http://dx.doi.org/10.1016/j.devcel.2015.05.024

CellPress

Please cite this article in press as: Elewa et al., POS-1 Promotes Endo-mesoderm Development by Inhibiting the Cytoplasmic Polyadenylation of *neg-1* mRNA, Developmental Cell (2015), http://dx.doi.org/10.1016/j.devcel.2015.05.024

Developmental Cell
Article

POS-1 Promotes Endo-mesoderm Development by Inhibiting the Cytoplasmic Polyadenylation of *neg-1* mRNA

Ahmed Elewa,[1,8,10] Masaki Shirayama,[1,8] Ebru Kaymak,[2] Paul F. Harrison,[3,4] David R. Powell,[3,4] Zhuo Du,[6] Christopher D. Chute,[7] Hannah Woolf,[1,9] Dongni Yi,[1] Takao Ishidate,[1] Jagan Srinivasan,[7] Zhirong Bao,[6] Traude H. Beilharz,[5] Sean P. Ryder,[2] and Craig C. Mello[1,*]

[1]Program in Molecular Medicine, RNA Therapeutics Institute and Howard Hughes Medical Institute, University of Massachusetts Medical School, 368 Plantation Street, Worcester, MA 01605, USA
[2]Department of Biochemistry and Molecular Pharmacology, University of Massachusetts Medical School, Worcester, MA 01605, USA
[3]Victorian Bioinformatics Consortium, Monash University, Clayton, Victoria 3800, Australia
[4]Life Sciences Computation Centre, Victorian Life Sciences Computation Initiative, Carlton, Victoria 3053, Australia
[5]Department of Biochemistry and Molecular Biology, Monash University, Clayton, Victoria 3800, Australia
[6]Developmental Biology Program, Sloan-Kettering Institute, New York, NY 10065, USA
[7]Department of Biology and Biotechnology, Worcester Polytechnic Institute, Life Science and Bioengineering Center, Gateway Park, 60 Prescott Street, Worcester, MA 01605, USA
[8]Co-first author
[9]Present address: The College of Arts and Sciences, Washington University in St. Louis, 1 Brookings Drive, St. Louis, MO 63130, USA
[10]Present address: Department of Cell and Molecular Biology, Karolinska Institutet, 17177 Stockholm, Sweden
*Correspondence: craig.mello@umassmed.edu
http://dx.doi.org/10.1016/j.devcel.2015.05.024

SUMMARY

The regulation of mRNA translation is of fundamental importance in biological mechanisms ranging from embryonic axis specification to the formation of long-term memory. POS-1 is one of several CCCH zinc-finger RNA-binding proteins that regulate cell fate specification during *C. elegans* embryogenesis. Paradoxically, *pos-1* mutants exhibit striking defects in endo-mesoderm development but have wild-type distributions of SKN-1, a key determinant of endo-mesoderm fates. RNAi screens for *pos-1* suppressors identified genes encoding the cytoplasmic poly(A)-polymerase homolog GLD-2, the Bicaudal-C homolog GLD-3, and the protein NEG-1. We show that NEG-1 localizes in anterior nuclei, where it negatively regulates endo-mesoderm fates. In posterior cells, POS-1 binds the *neg-1* 3′ UTR to oppose GLD-2 and GLD-3 activities that promote NEG-1 expression and cytoplasmic lengthening of the *neg-1* mRNA poly(A) tail. Our findings uncover an intricate series of post-transcriptional regulatory interactions that, together, achieve precise spatial expression of endo-mesoderm fates in *C. elegans* embryos.

INTRODUCTION

Eukaryotic cells exercise remarkable control over the post-transcriptional expression of mRNA. This is most notable in specialized cells such as large polarized embryonic cells and neurons, where a host of RNA-binding factors have been shown to regulate the spatial and temporal expression of mRNAs by controlling mRNA translation, stability, and localization within the cell (Darnell and Richter, 2012; Richter and Lasko, 2011). Translation efficiency for mRNAs is often positively correlated with poly(A) tail length, whereas tail shortening is frequently associated with mRNA turnover (Eckmann et al., 2011; Mangus et al., 2003). However, for some mRNAs, tail shortening does not lead to turnover but, instead, correlates with storage. Cytoplasmic poly(A) tail lengthening can restore translation of these stored mRNAs (Weill et al., 2012). The conserved cytoplasmic poly(A) polymerase GLD-2 has been implicated in lengthening poly(A) tails and activating the translation of mRNAs in the *C. elegans* germline (Wang et al., 2002), mouse and frog oocytes (Barnard et al., 2004; Kwak et al., 2004; Nakanishi et al., 2006), and *Drosophila* embryos (Cui et al., 2008).

GLD-2 polyadenylation of its targets is thought to be regulated through RNA-binding co-factors (D'Ambrogio et al., 2013). For example, in *C. elegans*, GLD-2 binds to the conserved K homology (KH) domain protein GLD-3, a homolog of *Drosophila* Bicaudal-C (Eckmann et al., 2004). GLD-3 stimulates GLD-2 activity in vitro (Wang et al., 2002). In addition, GLD-2 polyadenylation of *gld-1* mRNA requires both GLD-3 and the RNA-binding domain-containing protein RNP-8 (Kim et al., 2010). *gld-2* mutants are sterile, and, therefore, the role of this gene in poly(A) tail synthesis has been examined in the germline alone. The role of GLD-2, if any, in controlling mRNA translation in *C. elegans* embryos has not been studied.

Genetic studies have identified several mRNA binding factors that control cell fate specification during early *C. elegans* embryogenesis. These factors include the KH domain protein MEX-3 (Draper et al., 1996) and several tandem CCCH zinc-finger proteins related to the vertebrate Tis11 gene, including POS-1 and MEX-5 (Mello et al., 1992; Schubert et al., 2000; Tabara et al., 1999). Although a few target mRNAs for these factors

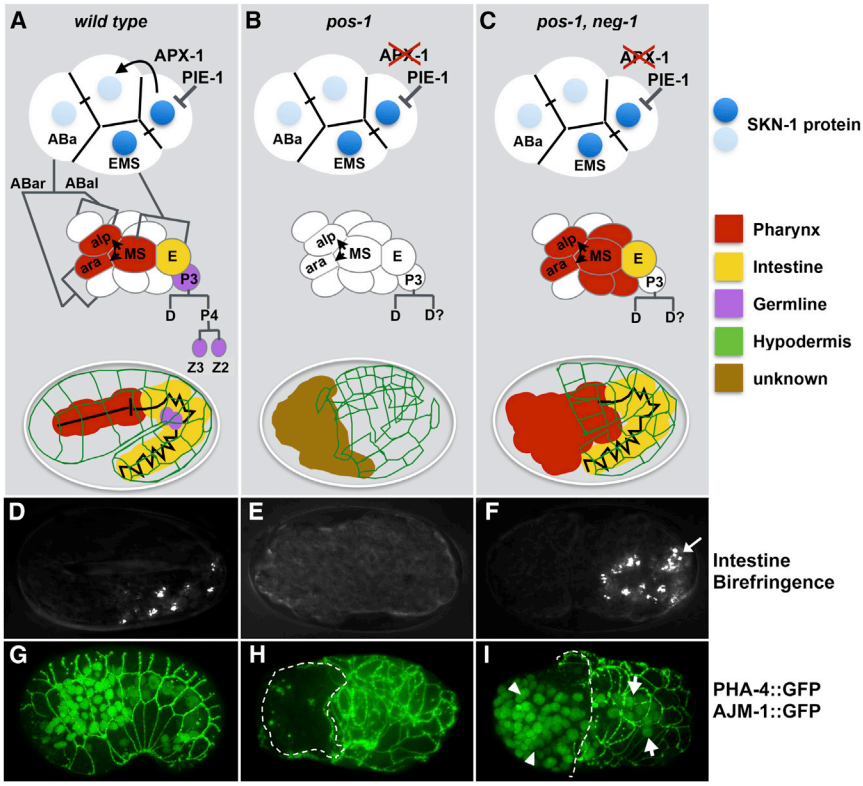

Figure 1. The *pos-1* Gutless Phenotype Is Suppressed by *neg-1* Loss of Function

(A–C) Schematic diagrams showing key features in endo-mesoderm differentiation in wild-type and mutant backgrounds (as indicated). At the four-cell stage (A), SKN-1 localization and APX-1 signaling restrict endo-mesoderm potential to the blastomeres EMS and ABa. At the 12-cell stage, MS signaling induces pharyngeal development in adjacent ABa descendants. Finally, body morphogenesis leads to enclosure of internal organs inside a network of hypodermal cells (shown in green). The germlineage P3 continues to divide asymmetrically, producing the germline precursors Z2 and Z3 (purple). Defects in these events are indicated in the mutant contexts (B and C).

(D–F) Polarized light micrographs showing gut differentiation as indicated by birefringent gut granule accumulation (D and F, absent in E).

(G) GFP fluorescence micrographs showing two differentiation markers: AJM-1::GFP, which is expressed at cell-cell junctions of epidermal cells surrounding the embryo (McMahon et al., 2001), and PHA-4::GFP, which is expressed in the nuclei of pharyngeal and intestinal precursors (Horner et al., 1998).

(H and I) Failure of the AJM::GFP network to enclose the anterior region of the embryo is indicated by a dashed line, and PHA-4::GFP nuclear staining, absent in (H), is restored in *pos-1, neg-1* double mutants (I, arrows).

have been identified, the targets, mechanism of regulation by RNA binding, and developmental outcomes remain largely unknown. For example, the tandem CCCH protein POS-1 is best studied for its role in restricting the translation of the GLP-1 mRNA to the anterior of the early embryo (Ogura et al., 2003). However, misregulation of GLP-1 (a Notch receptor homolog) cannot explain the nearly complete lack of endo-mesoderm specification observed in *pos-1* mutant embryos.

Here we explore the role of POS-1 in early embryonic events that specify endo-mesoderm precursor cells that give rise to the majority of the *C. elegans* alimentary canal, including the pharynx and intestine. The endo-mesoderm components of the *C. elegans* alimentary canal are specified through both cell-intrinsic and inductive mechanisms (Goldstein, 1992; Mello et al., 1994; Priess and Thomson, 1987). A major endo-mesoderm precursor cell named EMS produces the entire intestine and the posterior portion of the pharynx. EMS is born through two asymmetric divisions that sequentially segregate the potential to express endo-mesoderm fates to the posterior sister cell during the first division of the egg and then to the anterior sister cell during the second division (Figure 1A). The transcription factor SKN-1 is a major determinant of EMS development and accumulates asymmetrically in early four-cell stage embryos, where its levels become high in the posterior sister cells EMS and P2 (Bowerman et al., 1992). SKN-1 activity is further restricted to EMS through the activity of PIE-1, which localizes in the nucleus of P2, where it prevents SKN-1 from activating gene expression (Mello et al., 1992, 1996). In EMS, SKN-1 activates the expression of endo-mesoderm-promoting transcription factors, including MED-1, which promotes the expression of downstream genes required for EMS development (Maduro et al., 2001, 2007). Although POS-1 is critical for EMS specification, the expression and localization of SKN-1 protein is wild-type in *pos-1* mutant embryos, suggesting that POS-1 promotes EMS differentiation through other still unknown factors.

Here we identify GLD-2, GLD-3, and NEG-1 as factors whose loss of function restores endoderm differentiation in *pos-1* mutant embryos. We show that NEG-1::GFP accumulates asymmetrically to higher levels in the nuclei of anterior blastomeres of four-cell stage wild-type *C. elegans* embryos. GLD-2 and GLD-3 are required for NEG-1::GFP expression, whereas POS-1 is required to restrict the accumulation of NEG-1 protein to anterior blastomeres. We show that POS-1 binds directly to two consensus binding sites in the *neg-1* 3′ UTR and that POS-1 activity correlates with short *neg-1* mRNA poly(A) tails, whereas GLD-2 and GLD-3 activities correlate with long *neg-1* poly(A) tails. Moreover, we employ a deep sequencing approach, termed poly(A) Tail cDNA sequencing (PAT-seq), to analyze poly(A) tail length transcriptome-wide in early embryos. We identify numerous transcripts whose poly(A) tail lengths depend reciprocally on POS-1 activity and the activities of GLD-2 and GLD-3. Finally, we show that NEG-1 activity is required to prevent anterior blastomeres from ectopically expressing endo-mesoderm fates and that POS-1 restricts NEG-1 activity to ensure proper endo-mesoderm development in the posterior. Interestingly, the GLD-3 homolog Bicaudal-C antagonizes posterior development in the anterior of *Drosophila* embryos, suggesting that portions of this regulatory circuit are conserved across phyla.

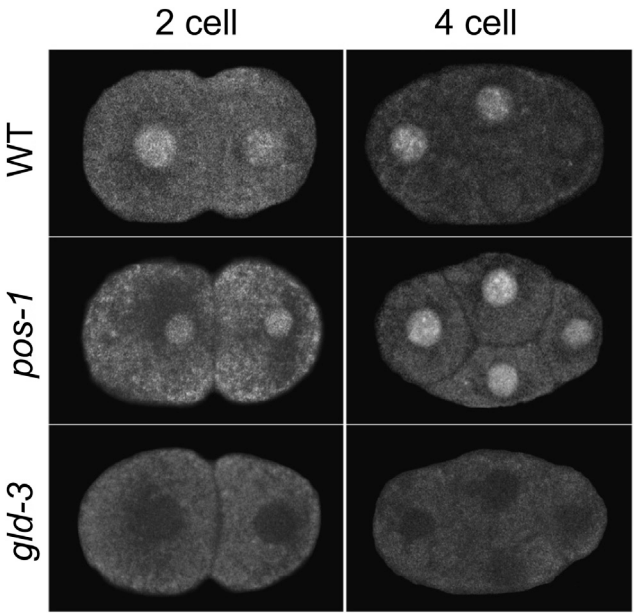

Figure 2. NEG-1::GFP Is Expressed Asymmetrically in the Early Embryo

Shown are representative confocal images of NEG-1::GFP rescuing *neg-1(tm6077)* in otherwise WT, *pos-1(zu148)*, and *gld-3(RNAi)* two-cell and four-cell embryos.

RESULTS

Restoration of the Gut in *pos-1* Embryos

Gut specification requires the activity of SKN-1 and a downstream gene regulatory network, including the GATA transcription factors MED-1 and END-1 (Bowerman et al., 1992; Maduro et al., 2007). SKN-1 protein levels and distribution are unaffected in the early blastomeres of pos-1 embryos (Tabara et al., 1999). Downstream transcription factors such as MED-1 and END-1, however, are not detected in the presumptive EMS lineage of *pos-1* embryos (data not shown). Moreover, analysis of the *med-1* mRNA by in situ hybridization revealed reduced levels of *med-1* mRNA relative to wild-type embryos (Figure S1A). Together, these findings suggest that, although SKN-1 is expressed and localized properly in *pos-1* mutants, it fails to initiate the gut developmental program. Consistent with this idea, we found that overexpression of the downstream transcription factor MED-1 using a multicopy transgenic array could bypass the *pos-1* gutless phenotype, restoring gut differentiation in 83% (618 of 762) of *med-1(+++); pos-1* embryos (compared with 2% [9 of 437] in *pos-1(zu148)* embryos).

Analysis of genetic interactions between *pos-1* and a panel of maternal RNA-binding proteins revealed that RNAi of the KH domain gene *gld-3* strongly suppresses the *pos-1* gutless phenotype (70.3% ± 11.6%, n = 144 embryos, and data not shown; Figures S1B and S1C). This suppression resulted in embryos with well differentiated endoderm and pharyngeal tissue but did not correct other defects, including the failure in *pos-1* mutants to properly specify the ABp fate through a GLP-1 mediated interaction and the failure to properly specify the germline cells Z2 and Z3. To search for additional factors whose loss of function could restore gut development in *pos-1* mutants, we used RNAi to systematically screen a set of 944 genes annotated previously as required for embryogenesis. Homozygous *pos-1* hermaphrodites were exposed to RNAi, and their embryos were then examined under a light microscope for intestinal birefringence (Experimental Procedures). We found that RNAi targeting seven different genes restored gut differentiation in the *pos-1* embryos (Table S1). In each case, as observed for *gld-3(RNAi)*, suppression of *pos-1* was limited to the restoration of endo-mesoderm differentiation, whereas proper ABp and P4 cell fates were not restored (see below and data not shown).

Among the genes identified in our screen were *gld-2*, which encodes a cytoplasmic poly(A) polymerase required for germline development, and F32D1.6, which encodes a protein with no obvious functional domains. We named this gene *neg-1* because of its negative effect on gut differentiation (note that, while this study was under preparation, another study identified a role for *neg-1* in anterior morphogenesis [Osborne Nishimura et al., 2015]). We found that knockdown of *gld-2* by RNAi resulted in sterility but that weak *gld-2(RNAi)* (Experimental Procedures) resulted in partial suppression of *pos-1* (41%, n = 38; Table S1). RNAi of *neg-1* caused a robust suppression of the *pos-1* endo-mesoderm differentiation defect (79%, n = 152; Table S1). Similarly, the *neg-1(tm6077)* mutation restored endo-mesoderm specification in *pos-1* mutant embryos to 74% (n = 293), suggesting that *neg-1(tm6077)* behaves like a loss-of-function mutation (Figures 1F and 1I). The 407 bp *neg-1(tm6077)* deletion removes approximately 60% of the of *neg-1* open reading frame, including the C-terminal 97 amino acids, and deletes a carboxy-terminal domain in the NEG-1 protein that is conserved in homologs found in related nematode species (Figure S5B).

POS-1 Restricts NEG-1::GFP Expression to Anterior Cell Lineages

GLD-2 and GLD-3 have been proposed to activate translation of target mRNAs by lengthening their poly(A) tails (Crittenden et al., 2003; Eckmann et al., 2004; Wang et al., 2002). Therefore, an attractive model is that GLD-2 and GLD-3 promote the expression of one or more endo-mesoderm antagonists and that POS-1 functions in endo-mesoderm lineages to oppose GLD-2 and GLD-3 activities. NEG-1 could function with GLD-2 and GLD-3 to promote the expression of such an antagonist. Alternatively, NEG-1 itself might be the hypothetical endo-mesoderm antagonist.

To begin to explore these possibilities, we engineered a strain expressing a single-copy full genomic fusion *neg-1::gfp* transgene (Frøkjaer-Jensen et al., 2008). Strikingly, we found that NEG-1::GFP is asymmetrically localized in the early embryo (Figure 2; Movie S1). NEG-1::GFP was detected in the zygotic nucleus and at equal levels in both nuclei of the two-cell embryo (23 of 23). However, at the four-cell stage, NEG-1::GFP expression was markedly higher in nuclei of the anterior AB blastomeres than in the nuclei of EMS and P2 (31 of 34). Following the four-cell stage, NEG-1::GFP remained high in the granddaughters of the AB blastomere and diminished progressively in subsequent divisions (data not shown). In the adult germline, we observed NEG-1::GFP in the nuclei of distal germ cells and the nuclei of growing oocytes except for the most proximal oocyte (Figure S2A). Moreover, we observed intense sub-nuclear localization of

NEG-1:GFP on condensed chromatin (11 of 11 NEG-1::GFP+ nuclei) (Figure S2B).

Next we examined the effect of POS-1, GLD-2, and GLD-3 activities on NEG-1::GFP expression. We found that the asymmetry in NEG-1::GFP expression was abolished in *pos-1* mutant embryos (Figure 2). Instead, NEG-1::GFP was expressed at high levels characteristic of AB descendants in all lineages of the *pos-1(RNAi)* (14 of 14) and *pos-1(zu148)* (6 of 6) embryos examined. In contrast, we found that NEG-1::GFP expression was absent or greatly reduced at all embryonic stages in *gld-2*- and *gld-3*-depleted embryos (Figure 2; data not shown). As expected, we found that *gld-3* is epistatic to *pos-1*. NEG-1::GFP expression, including its ectopic expression in EMS and P2, was abolished in *pos-1; gld-3* double mutants (n = 6). Taken together, these findings suggest that POS-1 represses the expression of NEG-1 in posterior blastomeres, whereas GLD-2 and GLD-3 are required to promote NEG-1 expression.

Consensus POS-1 Binding Elements Are Required for NEG-1 Asymmetry

Early *C. elegans* embryos are transcriptionally quiescent (Guven-Ozkan et al., 2008; Seydoux and Dunn, 1997), and, therefore, regulation of NEG-1::GFP likely occurs at the level of mRNA translation or protein stability. To ask whether NEG-1 expression is regulated through the 3′ UTR of the *neg-1* mRNA, we fused *gfp* containing a nuclear localization sequence to the 3′ UTR of *neg-1* (hereafter called *gfp*::3′UTR^{neg-1}) and placed this reporter under the promoter of the maternally expressed gene *oma-1* (Experimental Procedures). We found that the pattern of GFP expression from this reporter, which entirely lacks *neg-1* coding sequences, was identical to that of the full-length *neg-1::gfp* fusion gene (Figure S3A; Movie S2). We therefore conclude that the 3′ UTR of *neg-1* is sufficient to confer asymmetric expression in the early embryo.

The 3′ UTR of *neg-1* contains three overlapping, predicted RNA binding protein (RBP) elements, referred to here as the RBP cluster (Figure 3A). This RBP cluster begins with a uracil-rich sequence that represents a consensus MEX-5 binding region that is adjacent to overlapping MEX-3 and POS-1 predicted binding elements (Farley et al., 2008; Pagano et al., 2007, 2009). To address whether MEX-3, MEX-5, and POS-1 physically bind to the RBP cluster, we carried out electrophoretic mobility shift assays (EMSAs) and fluorescence polarization (FP) assays (Experimental Procedures). We found that POS-1, MEX-3, and MEX-5 bind the RBP cluster with affinities comparable with those determined previously between each protein and confirmed biological targets (Figures 3B and 3C) and that MEX-5 binding to the RBP is favored over POS-1 binding (Figure S3B). Moreover, POS-1 binding was reduced when its putative binding site was mutated (Figures 3B and 3C; Figure S3B). In addition to binding within the RBP cluster, we found that MEX-5 binds a second region (M5B; Figures 3A and 3C). We also tested an additional region 3′ of the RBP cluster (P1M3B) that contains a consensus POS-1 binding element and an overlapping MEX-3 consensus sequence (Figure 3A) and found that both recombinant proteins bind this site with high affinity in vitro (Figures S3C and S3D).

To determine whether these consensus binding elements direct the in vivo regulation of NEG-1 expression, we generated *gfp*::3′UTR^{neg-1} reporters containing the same mutations as those used for the in vitro binding assays. We found that mutation of the predicted POS-1 binding element within the RBP cluster caused a more symmetric distribution of NEG-1::GFP between anterior and posterior blastomeres (Figure 3D, column PBE1). Combining this lesion with a lesion in the second POS-1 binding element, P1M3B, completely abolished the anterior-posterior asymmetry in NEG-1::GFP levels (Figure 3D, column PBE1&2). Interestingly, this double binding site mutant consistently exhibited NEG-1::GFP expression that, although equal between anterior and posterior blastomeres, was also lower in intensity than levels observed in wild-type anterior nuclei (data not shown), suggesting that one or both of these 3′ UTR elements may also contribute positively to NEG-1 expression.

mex-5 Positively Regulates *neg-1* Expression

MEX-5 and MEX-3 are enriched in anterior blastomeres (Draper et al., 1996; Schubert et al., 2000), where NEG-1 protein levels are high. Moreover, as shown above, these factors bind in vitro to regions in the NEG-1 3′ UTR that are also bound by POS-1 protein, raising the possibility that MEX-5 and MEX-3 are positive regulators of NEG-1 expression that directly compete with POS-1 for binding. Consistent with this possibility, we found that RNAi of *mex-5* and *mex-3* reduced the levels of NEG::GFP expression. In the case of *mex-3(RNAi)*, the asymmetry of NEG-1::GFP expression was not affected, but the overall levels appeared to be reduced slightly (Figure 3E; data not shown). Strikingly, however, RNAi knockdown of *mex-5* completely abolished NEG-1::GFP expression (0 of 30; Figure 3E). RNAi of *mex-6*, a partially redundant paralog of *mex-5*, did not affect NEG-1::GFP expression (data not shown). The complete absence of NEG-1 expression in *mex-5(RNAi)* early embryos is opposite to the consequence of *pos-1* loss of function. We therefore examined the consequences of *mex-5* knockdown in a *pos-1(zu148); neg-1::gfp* strain. We found that all *pos-1(zu148); mex-5(RNAi)* early embryos exhibited bright NEG-1::GFP expression characteristic of *pos-1* mutants (n = 14), including equal and high levels of NEG-1::GFP in all blastomeres at the four-cell stage (n = 4; Figure 3E). Similar results were obtained from *pos-1(RNAi); mex-5(RNAi)* double knockdown embryos (Figure 3E). These findings indicate that *pos-1* is epistatic to and genetically downstream of *mex-5* for the regulation of *neg-1* expression and suggest that MEX-5 protein promotes *neg-1* expression in the anterior by countering POS-1 repression. A previous study has shown that the POS-1 protein exhibits wild-type localization in *mex-5* mutant embryos (Tenlen et al., 2006), suggesting that the absence of *neg-1* in *mex-5(RNAi)* embryos is not caused by ectopic anterior accumulation of POS-1 protein. The finding that in vitro binding sites for MEX-3, MEX-5, and POS-1 overlap suggests that direct competition between these positive and negative factors may contribute to NEG-1 regulation and may also explain why mutating these elements abolishes both the asymmetry and the overall level of NEG-1::GFP expression.

POS-1, GLD-2, and GLD-3 Regulate *neg-1* Poly(A) Tail Length

In the germline, GLD-2 and GLD-3 are thought to positively regulate gene expression by promoting the cytoplasmic polyadenylation of target mRNAs (Crittenden et al., 2003; Eckmann et al.,

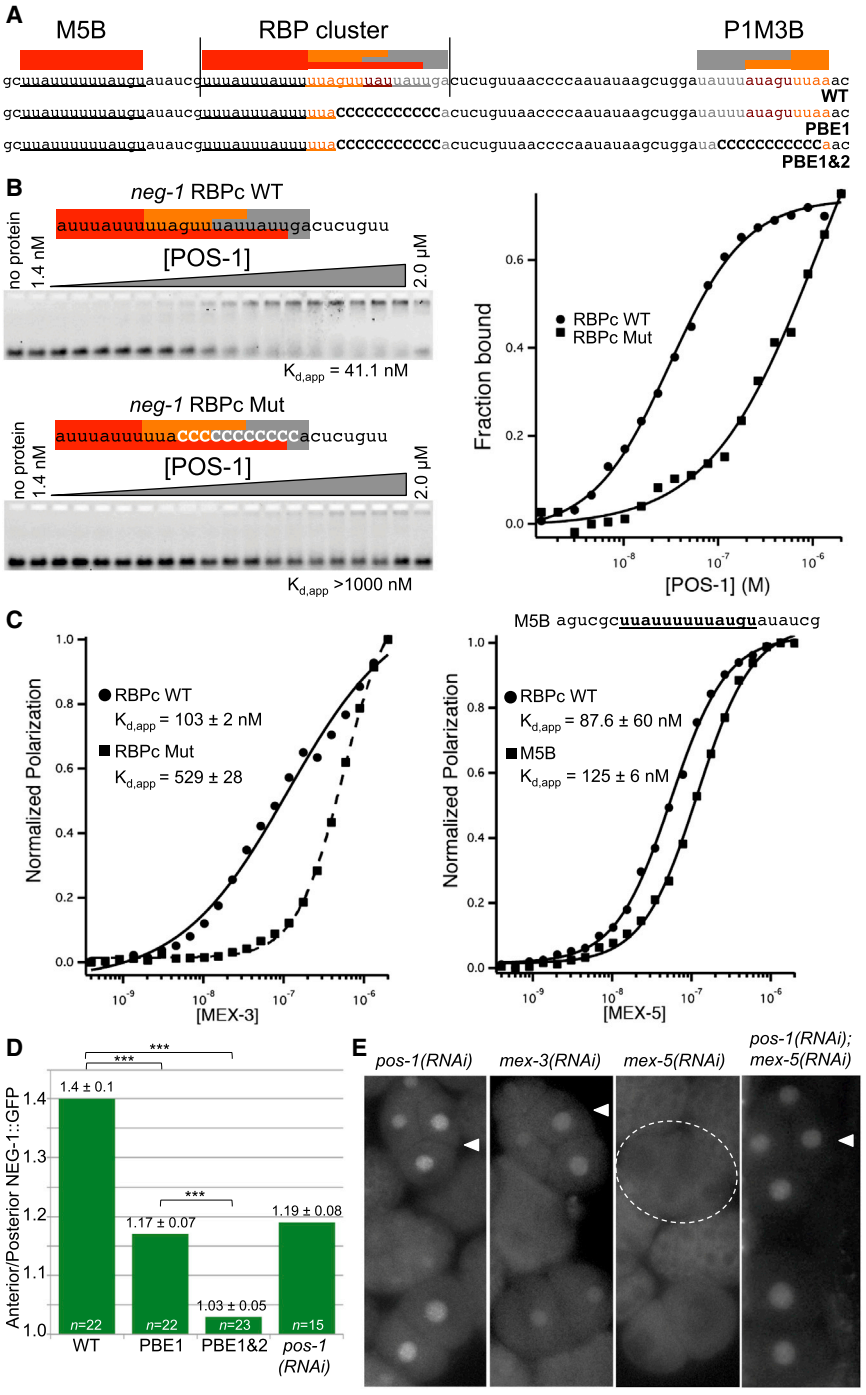

Figure 3. POS-1 and MEX-5 Bind and Regulate the Expression of *neg-1* mRNA

(A) Nucleotide sequence of a portion of the *neg-1* mRNA 3′ UTR indicating predicted binding sites for POS-1 (gray), MEX-3 (orange), and MEX-5 (red). WT and two sequences with mutations in the POS-1 consensus elements (PBE1 and PBE1&2) are shown.

(B) Fluorescence EMSAs with recombinant POS-1 and fluorescently labeled wild-type (RBPc WT) and mutant (RBPc Mut) fragments of the *neg-1* RBP cluster (as indicated). The mobility of each labeled probe is shown after incubation with increasing amounts of POS-1 protein, as indicated at the top of the gel images. The apparent dissociation constant, $K_{D,app}$, indicated below the gel images, represents the average of three independent replicates ± SD. A graphical quantification of the data is shown at the right.

(C) Graphical representations of fluorescence polarization data obtained from incubating the fluorescent probes (as indicated) with increasing amounts of MEX-3 (left) or MEX-5 (right). The RBP cluster probes were the same as those used in (B). The sequence of the MEX-5 B probe (M5B) is shown above the right graph. The $K_{D,app}$ values were calculated as described in (B).

(D) Graphical representation of relative anterior/posterior GFP intensity observed in four-cell stage embryos transgenic for *neg-1* promoter-driven GFP under the control of the *neg-1* WT or the mutated *neg-1* 3′ UTR. The mutations in the PBE1 and PBE1&2 UTRs are shown in (A). Relative anterior/posterior GFP intensity after *pos-1(RNAi)* is also indicated for comparison. The y axis indicates the average ratio of GFP intensity in the anterior (ABa + ABp) divided by intensity in the posterior (EMS + P2) (Experimental Procedures). Data are represented as mean ± SD. ***$p < 0.0001$. Sample size (*n*) is indicated for each column.

(E) GFP fluorescence micrographs showing the expression of a wild-type NEG-1::GFP reporter in representative wild-type embryos (WT) and embryos depleted by RNAi of various RBPs (as indicated).

2004; Wang et al., 2002). Indeed, several *C. elegans* transcripts expressed in the germline have been shown to be dependent on GLD-2 for their polyadenylation (Jänicke et al., 2012; Kim et al., 2010). Moreover, the *neg-1* transcript is one of hundreds of transcripts that have shortened poly(A)-tails in the sterile *gld-2* adult compared with wild-type adults (T.H.B., unpublished data). We therefore asked whether GLD-2 and GLD-3 might exert their positive effects on NEG-1 expression by promoting the polyadenylation of *neg-1* mRNA in the embryo.

To measure the length of *neg-1* poly(A) tails in early embryos, we used a deep sequencing approach termed PAT-seq (Experimental Procedures; T.H.B., P.F.H., and D.R.P., unpublished data). If NEG-1 regulation is achieved through polyadenylation, then NEG-1 would be expected to have long poly(A) tails in anterior blastomeres and short tails in posterior blastomeres. If this difference in poly(A) tail length between blastomeres is significantly large, we would detect two different populations of tail lengths when analyzing whole embryos. Consistent with this idea, we observed a bimodal distribution of *neg-1* poly(A) tail lengths in wild-type embryos (Figure 4A), with a clustering of longer tails centered at around 80 A residues and a second clustering of shorter tails centered at approximately 20 A residues in length (Figure 4B) (n = 318 tails). In *pos-1* mutants, the

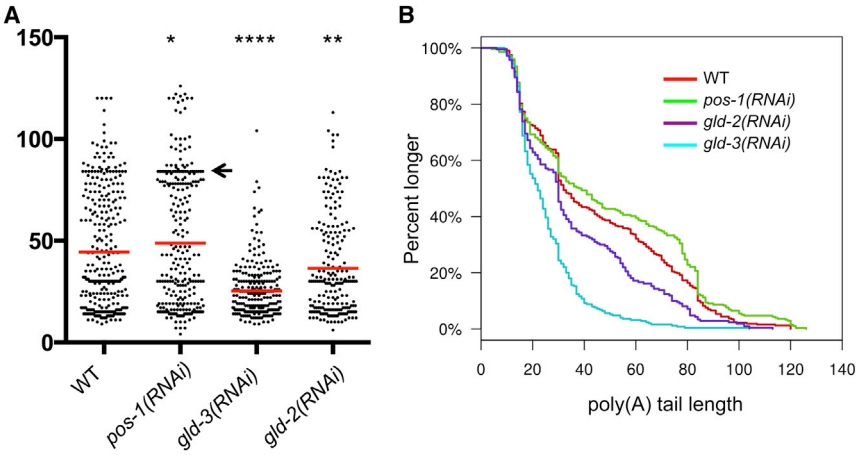

Figure 4. POS-1, GLD-3, and GLD-2 Regulate *neg-1* mRNA Poly(A) Tail Length

(A) Graphical representation of *neg-1* mRNA poly(A) tail lengths as detected by PAT-seq analysis of RNA prepared from WT and mutant early embryos (as indicated). Each dot represents a cDNA sequence and the number A residues in its poly(A) tail corresponding to its placement on the y axis. A high density of dots may appear as a black line. The red bar reflects the median according to Kolmogorov-Smirnov test. *p $\leq$ 0.05, **p $\leq$ 0.01, ****p $\leq$ 0.0001. The arrow denotes a range of overrepresented poly(A) tail lengths in the WT that increases in *pos-1(RNAi)* early embryos.

(B) A continuous histogram demonstrating the percentage of poly(A) tails (y axis) longer than a given length (x axis) in each genotype tested.

density of reads with approximately 80 A residues was increased and was more tightly clustered relative to the wild-type (WT) (Figures 4A, arrow, and 4B). Furthermore, the median poly(A) read length was increased slightly (red bars in Figure 4A), as was the average from 44.4 bases in the WT to 48.9 bases in *pos-1* (n = 276 tails, p = 0.05). In contrast, read lengths were shifted dramatically toward shorter tails in *gld-3* and *gld-2* depleted embryos (Figures 4A and 4B), with an average length in *gld-3(RNAi)* embryos of 25.3 (n = 250 tails, p = 0.00005) and in *gld-2(RNAi)* embryos of 36.3 (n = 210 tails, p = 0.005). Taken together, these findings suggest that POS-1 and GLD-2/GLD-3 regulate the expression of NEG-1 by controlling the polyadenylation status of *neg-1* mRNA.

neg-1(+) Activity Represses Anterior Endo-mesoderm Differentiation

To further analyze the function of *neg-1,* we characterized the loss-of-function phenotypes associated with *neg-1(RNAi)* or the deletion allele *neg-1(tm6077)*. Interestingly, we found that *neg-1*, like *pos-1,* is required maternally for proper embryonic development. Approximately 75% of embryos produced by the homozygous *neg-1* mutant (or RNAi) mothers die before hatching. In most cases, the dead embryos exhibit defective morphogenesis, characterized by a failure of hypodermal cells to properly enclose the anterior portion of the embryo (Figure 5A). These findings suggest that *neg-1(+)* activity promotes anterior cell fate specification and/or morphogenesis.

Because *neg-1* is an antagonist of gut specification, we wondered whether NEG-1 might function during wild-type development to represses mesoderm or endoderm differentiation in lineages that normally specify portions of the anterior hypodermis. To explore this possibility, we examined the expression pattern of PHA-4 in *neg-1(tm6077)*. *pha-4* encodes a FoxA transcription factor expressed in mesodermal and endodermal precursor cells (Du et al., 2014; Horner et al., 1998). Using 4D microscopy to trace lineages (Hardin, 2011), we found that PHA-4::GFP was expressed ectopically in anterior AB sub-lineages of *neg-1(tm6077)* embryos, suggesting that NEG-1 prevents PHA-4 expression in lineages that are normally destined to become ectoderm (Figures 5B and 5C; Figure S4).

In addition to hypodermal lineages, *neg-1* loss of function also affects neuronal lineages. We therefore analyzed *neg-1* mutants that survived embryogenesis for behavioral deficits that might reflect impaired neuronal function. We found that *neg-1* worms exhibit reduced osmotic avoidance. Wild-type L4 worms avoided 2 M glycerol with an avoidance index of 0.63 ± 0.05 (n = 80), whereas *neg-1* worms of the same stage scored 0.33 ± 0.06 (n = 60) (Figure 5E).

As described above, we found that overexpression of the endo-mesoderm promoting transcription factor *med-1* can partially suppress the *pos-1* gutless phenotype. We reasoned, therefore, that *med-1* loss of function might suppress ectopic mesoderm differentiation and restore anterior development in *neg-1* embryos. Indeed, we found that *med-1(ok804)* dramatically reduced embryonic lethality of *neg-1(tm6077)* from ~75% to 35.6% ± 13.3% (n = 1,545 embryos; Figure 5D). Notably, the osmotic avoidance defect of *neg-1* was also suppressed (0.68 ± 0.06, n = 60; Figure 5E), suggesting that ectopic mesoderm differentiation also causes the *neg-1* behavioral phenotype. Taken together, these findings suggest that NEG-1 functions in the anterior to ensure robust ectoderm specification, at least in part, by preventing endo-mesoderm development and that POS-1 promotes posterior endo-mesoderm differentiation by restricting NEG-1 protein accumulation to the anterior.

DISCUSSION

Early embryonic patterning in *C. elegans* involves the precise spatial and temporal control of mRNA translation (Begasse and Hyman, 2011). Maternal mRNAs encoding transcription factors, cell signaling components, and other developmental regulators become differentially expressed in early embryonic cells, contributing to the rapid diversification of cell fates (Hwang and Rose, 2010). Here we explored the role of the RNA-binding protein POS-1 in this process. We have shown that a maternal mRNA encoding an endo-mesoderm repressor NEG-1 is a key target for POS-1 regulation. Taken together, our genetic, molecular, and localization studies support a model in which POS-1 binds to the *neg-1* mRNA and regulates its cytoplasmic poly-adenylation (Figure 6A). Our findings suggest that POS-1 and its homolog MEX-5 bind adjacent sequences in the *neg-1* mRNA 3′ UTR and have opposing effects on the recruitment of the cytoplasmic poly(A) polymerase GLD-2 and its co-factor GLD-3. In anterior blastomeres, where MEX-5 levels are high (Schubert

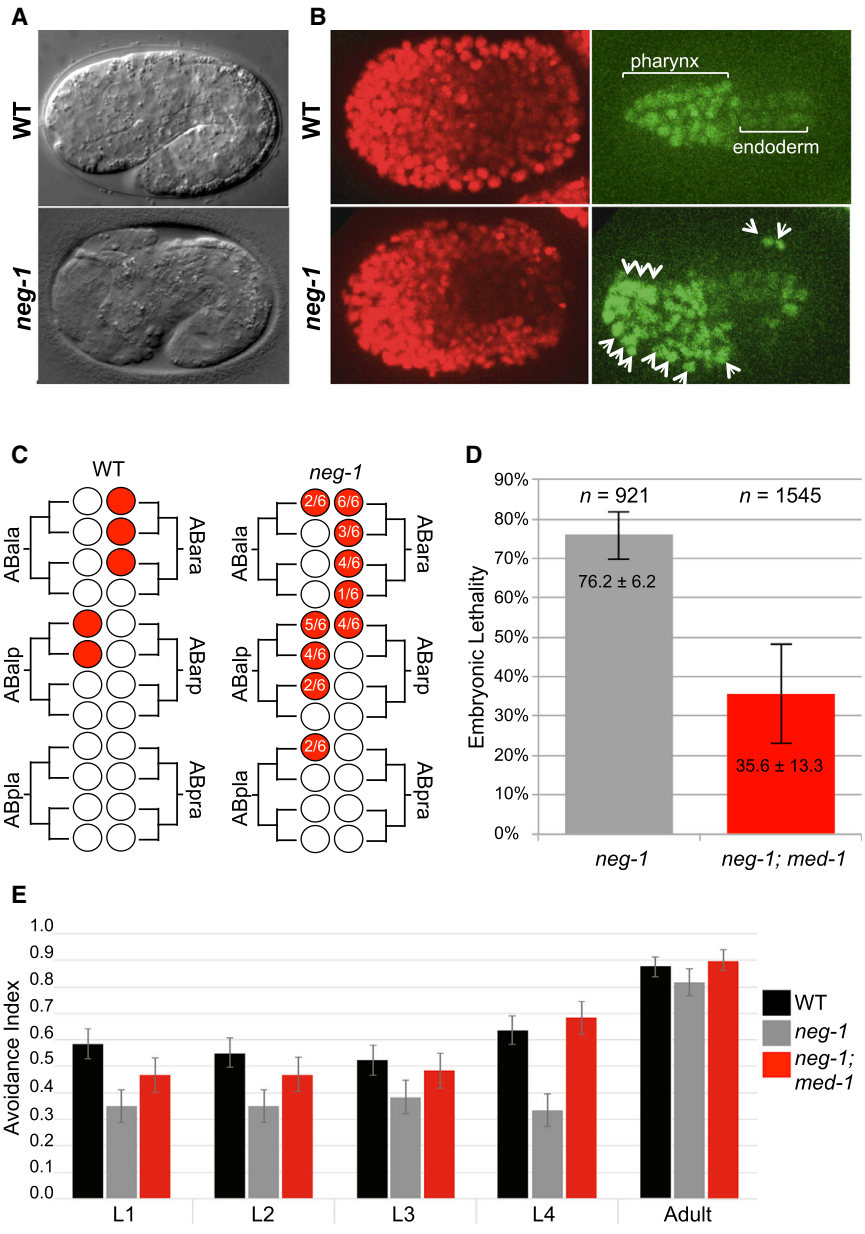

Figure 5. *neg-1* Prevents Ectopic Endo-mesoderm Differentiation in the AB Lineage

(A) Nomarski light micrographs showing wild-type and *neg-1* embryos approximately midway through body morphogenesis. The defective anterior enclosure with resulting external pharyngeal tissue (white arrows) is indicated in the *neg-1* embryo.

(B and C) Ectopic PHA-4::GFP expression in *neg-1(−)* embryos.

(B) Fluorescence micrographs of a WT and *neg-1(tm6077)* embryo expressing *histone::mCherry* (marking all nuclei) and *pha-4::gfp* (marking pharyngeal and endodermal cells). The white arrowheads indicate ectopic pharyngeal cells in the *neg-1* embryo.

(C) Lineage diagrams constructed from 4D microscopy studies on six independently analyzed *neg-1(tm6077)* embryos. Wild-type lineages that produce a pharynx are shown by red circles in the diagram at the left. The *neg-1* lineages that were positive for PHA-4::GFP are shown at the right, with the frequency of GFP detection indicated inside each red circle. The diagram is a summary of the lineages in Figure S4.

(D and E) *med-1* loss of function suppresses *neg-1* mutant phenotypes.

(D) Bar graph showing the percent embryonic lethality in *neg-1(tm6077)* single mutant and *neg-1(tm6077); med-1(ok804)* mutant embryos (as indicated; n = number of embryos assayed). The error bars indicate the mean ± SD.

(E) Bar graph showing the glycerol avoidance index for the wild-type (n = 80) and the *neg-1(tm6077)* (n = 60) and *neg-1(tm6077); med-1(ok804)* (n = 60) double mutant strains (as indicated). The larval stages analyzed, L1 through adult, are indicated. The avoidance index is calculated as the number of positive responses divided by the total number of trials (see text) ± SEM.

et al., 2000), MEX-5 overcomes POS-1 inhibition, leading to GLD-2/GLD-3 recruitment, extension of *neg-1* poly(A) tails, and accumulation of NEG-1 protein, which, in turn, represses endo-mesoderm fates, ensuring the proper expression of ectodermal (skin and neuronal) cell fates. Conversely, in posterior blastomeres, high POS-1 levels prevent GLD-2/GLD-3-mediated activation of *neg-1* mRNA translation and, therefore, protect endo-mesoderm precursors from NEG-1 protein accumulation (Figure 6B).

GLD-2 and GLD-3 as Regulators of Early Embryogenesis

Previous work has demonstrated that GLD-2 and GLD-3 function together during germline development to promote the transition from mitosis to meiosis (Crittenden et al., 2003; Eckmann et al., 2004; Wang et al., 2002). Here we have shown that GLD-2 and GLD-3 also promote embryogenesis by positively regulating the expression of the endo-mesoderm inhibitor NEG-1. Our findings suggest that GLD-2 and GLD-3 promote NEG-1 expression by lengthening the poly(A) tail of *neg-1* mRNA. Similar regulatory interactions may control the expression of other proteins that accumulate in anterior blastomeres. Of more than 5,000 genes represented in our early embryo PAT-seq datasets, we identified 436 with "GLD-2/GLD-3-activated, POS-1-repressed" poly(A) tail lengths (Figure 6C). These included *mex-3*, *mex-5*, *mex-6*, and *zif-1*, whose protein products are enriched in the anterior in a pattern similar to that of NEG-1 (DeRenzo et al., 2003; Draper et al., 1996; Schubert et al., 2000). A recent study used oligo-dT selection to recover mRNAs from isolated anterior and posterior blastomeres of two-cell-stage *C. elegans* embryos (Osborne Nishimura et al., 2015). Interestingly, comparing these data to our PAT-seq data revealed that 40.5% (17 of 42) of the AB-enriched mRNAs from the single-blastomere study, but only 1.8% (2 of 112) of P1-enriched mRNAs, were among the

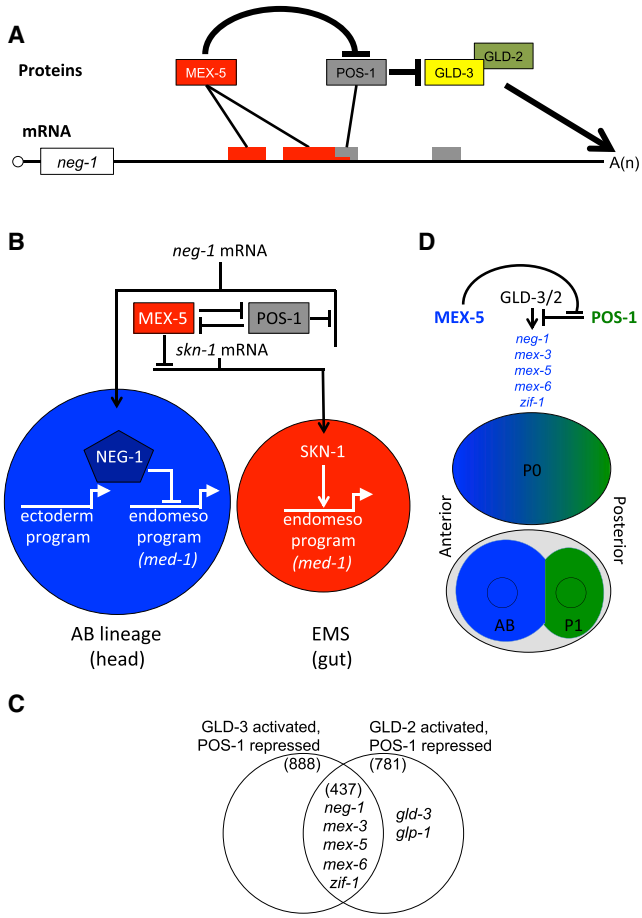

Figure 6. RBPs Control Cytoplasmic Polyadenylation of mRNAs to Establish Anterior-Posterior Asymmetries

(A) Molecular regulation of *neg-1* expression. MEX-5 and POS-1 bind the 3′ UTR of *neg-1*. POS-1 prevents GLD-3/2 polyadenylation of *neg-1* in posterior lineages, and MEX-5 counters POS-1 repression in anterior lineages.

(B) Model for the regulation of cell fate specification in anterior and posterior lineages (blue and red circles, respectively). The diagram indicates how the regulation of mRNA translation by the RBPs POS-1 and MEX-5 ensures the asymmetric accumulation of the endo-mesoderm activator (SKN-1) and of the endo-mesoderm antagonist (NEG-1) and how the downstream activities of these factors ensure the proper expression of ectodermal and endo-mesodermal transcriptional programs. MEX-5-negative regulation of SKN-1 and POS-1 is based on Schubert et al. (2000).

(C) GLD-2/GLD-3-activated, POS-1-repressed genes are those that had shorter tails upon *gld-3* RNAi or *gld-2* RNAi and longer poly(A) tails after *pos-1* RNAi (overlap between both circles). This common group consists of 436 genes that include the anterior expressed *neg-1*, *mex-3*, *mex-5*, *mex-6*, and *zif-1*. *gld-3* and *glp-1* qualify as GLD-2-activated, POS-1-repressed genes but not as GLD-3-activated, POS-1-repressed genes.

(D) Model indicating how the regulatory circuit that controls *neg-1* mRNA expression may also explain the regulation of many other mRNAs, including those of several genes studied previously (indicated).

GLD-2/GLD-3-activated, POS-1-repressed group of mRNAs identified by PAT-seq (Tables S2 and S3). These findings suggest that the POS-1/GLD-2/GLD-3 interactions that regulate *neg-1* poly(A) tail length may also function more generally to regulate the asymmetric expression of dozens of target mRNAs, including *neg-1*, *zif-1*, and *mex-3/5/6* (Figure 6C).

It is not yet known how GLD-2 and GLD-3 are recruited to their targets. A structural study indicates that domains KH2-KH5 of GLD-3 assemble a thumb-like structure that may present KH1 for direct contact with GLD-2 (Nakel et al., 2010; Eckmann et al., 2004). These findings raise the question of whether GLD-3 can bind both mRNA and GLD-2 simultaneously and suggest that, rather than directly binding RNA to recruit GLD-2, GLD-3 may serve as an adaptor protein for GLD-2 recruitment by other RNA-binding factors. One attractive possibility is that CCCH-finger proteins contribute RNA-binding specificity that determines which mRNAs are targeted for poly(A) tail lengthening by GLD-2. With at least seven CCCH proteins (MEX-1, POS-1, MEX-5, MEX-6, OMA-1, OMA-2, and PIE-1) implicated in cell fate determination in early embryos, the combinatorial complexity available for mRNA regulation is substantial. Hinting at additional complexity, our findings reveal a subset of mRNAs whose poly(A) tail lengths appear to depend on GLD-2 but not GLD-3 activity (Figure 6D). Among these, the *glp-1* mRNA has been shown previously to be a target of POS-1-negative regulation in the posterior of the embryo (Ogura et al., 2003). It will therefore be interesting to determine whether a distinct GLD-2 complex that does not include GLD-3 activates GLP-1 mRNA translation. It is also worth noting that the mRNA of the GLP-1 ligand APX-1, whose protein expression in the P2 blastomere depends on POS-1(+) activity, is among a subset of mRNAs whose poly(A) tail lengths were correlated positively with GLD-2 and POS-1 (but not GLD-3 activity) (Table S3). Therefore, in addition to its role as a negative regulator of *neg-1* mRNA, POS-1 may function as a positive regulator that recruits a distinct GLD-2 complex to promote the lengthening of *apx-1* mRNA poly(A) tails.

A Conserved Mechanism for Regulating Anterior-Posterior Asymmetries?

How NEG-1 represses endo-mesoderm genes remains unclear. NEG-1 does not contain recognizable sequence domains that resemble other known functional elements, and only two homologs have been identified in related nematodes (Figures S5A and S5B). However, the nuclear localization of NEG-1 protein and its association with chromatin suggest that NEG-1 may prevent the activation of endo-mesoderm differentiation by acting as a transcriptional repressor.

Despite the absence of sequence homologs in other organisms, our findings suggest that NEG-1 partakes in a conserved mechanism that controls embryonic asymmetry in metazoans. *Drosophila* Bicaudal-C is required to prevent posterior (caudal/abdominal) fates from appearing ectopically in the anterior of the *Drosophila* embryo, a developmental function very similar to that described here for *C. elegans gld-3*. Interestingly, *Drosophila* Bicaudal-C appears to bind its own mRNA and repress translation by recruiting components of a conserved mRNA deadenylase complex (Chicoine et al., 2007). A recent study suggests that the *Xenopus* homolog Bic-C represses the expression of specific mRNAs in the vegetal hemisphere of early embryos by directly binding the translational control element present in their 3′ UTRs (Zhang et al., 2014). How these repressive functions of Bic-C proteins can be reconciled with our findings that GLD-3 functions to promote mRNA poly(A) tail length and gene expression remains to be seen. However, a dynamic

interplay between activities that shorten and lengthen poly(A) tails in the cytoplasm is thought to be central to the regulation of mRNA translation during fly oogenesis and *Xenopus* oocyte maturation (Ivshina et al., 2014). It is possible, therefore, that Bic-C proteins mediate repression by shortening poly(A) tails to promote mRNA turnover or to promote the storage of certain mRNAs for later activation. Conversely, by engaging GLD-2 protein, Bic-C proteins may have the ability to reverse this repression, selectively re-activating specific mRNAs. Currently we do not know how *neg-1* mRNA becomes de-adenylated. Therefore, it will be interesting to determine whether GLD-3 plays a role in recruiting a deadenylase complex to the *neg-1* mRNA, perhaps during oogenesis, to set the stage for re-adenylation later during embryogenesis.

In both fly and frog oocytes, conserved RNA binding factors called cytoplasmic polyadenylation element-binding proteins (CPEBs) play a key role in recruiting the cytoplasmic poly(A) polymerase GLD-2 to specific targets (Barnard et al., 2004; Benoit et al., 2008; Cui et al., 2008). Although CPEB proteins are conserved in *C. elegans* and have been shown to function with GLD-2 to regulate germline development, we have not found a role for CPEBs in regulating *neg-1* mRNA polyadenylation or other embryonic events. Perhaps POS-1 and its CCCH zinc-finger homologs provide RNA-binding and regulatory activities in *C. elegans* that are analogous to those provided by CPEB proteins in other organisms. There is clearly a rich complexity of mRNA regulation in metazoan embryos, especially in embryos where important early developmental events occur prior to the onset of zygotic transcription. It will be interesting in the future to determine the extent to which cytoplasmic polyadenylation and the rich combinatorial complexity of RNA-binding factors contribute to the remarkable unfolding of early embryonic patterning, organogenesis, and neurogenesis across phyla.

EXPERIMENTAL PROCEDURES

Strains

JJ462: +/nT1 IV; pos-1(zu148) unc-42(e270)/nT1 V.

WM317: *neg-1(tm6077)*. The deletion was obtained by the National Bioresource Project (Mitani Laboratory) and removed a region encoding the last 97 amino acids as well as the terminating stop codon of the gene, therefore fusing the coding region with the 3′ UTR and adding 11 codons to the predicted gene product before encountering an in-frame stop codon.

RW10425: stIs10116 [his-72(promoter)::his-24::mCherry + unc-119(+)]. stIs37 [pie-1(promoter)::mCherry::H2B + unc-119(+)]. stIs10389 [pha-4::GFP::TY1::3xFLAG].

WM310: *gfp::neg-1; neg-1(tm6077).* A region of cosmid F32D1 flanked by AflII and NotI digestion sites was subcloned, and an open reading frame (ORF) encoding GFP was introduced upstream of F32D1.6 *(gfp::neg-1).* The engineered transgene preserved *neg-1* in its predicted operon and its downstream neighbor *fipp-1* and was introduced using MosSCI transgenesis (Frøkjaer-Jensen et al., 2008). *gfp::neg-1* was crossed into the *neg-1(tm6077)* background.

WM311: *oma-1* promoter::NLS::*gfp*::*neg-1* 3′UTR (J608.6).

WM312: *oma-1* promoter::NLS::*gfp*::*neg-1* 3′ UTR with a mutated POS-1 binding site (see RBPc Mut in Table S2).

WM316: neg-1(tm6077); med-1(ok804).

WM326: pos-1(zu148) unc-42 (e230) /hT1 [med-1::gfp, rol-6(su1006)].

WM319: *oma-1* promoter::NLS::*gfp*::*neg-1* 3′ UTR with two mutated POS-1 binding elements.

med-1 In Situ Hybridization

In situ hybridization was performed as described by Tabara et al. (1999). Probes were designed against *gfp* mRNA and used to identify *med-1::gfp* in the strain *med-1::gfp, rol-6(su1006)* (Maduro et al., 2001) before and after *pos-1(RNAi)*.

pos-1 Suppressor Screen

The *pos-1* suppressor screen was performed by placing five to ten L2–L4 *pos-1(zu148) unc-42(e270)* worms on RNAi food and allowing them to reach adulthood and lay eggs. Embryos were then scored for gut granules. Positive hits were then retested by scoring the embryos (E) of four to six individual worms (*n*) fed the RNAi food to assess overall gut development and obtain average *pos-1* suppression and SD. The same protocol was followed for *gld-3* and *gld-2* suppression. For the effect of *med-1* upregulation, a *med-1::gfp* multicopy transgenic array was crossed with *pos-1(zu148) unc-42(e270)*, and embryos of homozygous hermaphrodites were scored for gut granules.

Binding Assays

Fluorescence anisotropy and EMSAs using purified recombinant POS-1 (80–180), MEX-3 (45–205) and MEX-5 (236–350) were done as described by Farley et al. (2008) and Pagano et al. (2007, 2009), respectively. All RNA oligonucleotides used in this study were chemically synthesized and fluorescently labeled at the 3′ end with fluorescein amidite (FAM) by Integrated DNA Technologies.

Competition assays were set up similar to the EMSAs. 550 nM of POS-1 (80–180) or 450 nM MEX-5 (236–350) was added to the RNA equilibration buffer to obtain a 70% RNA-bound complex. Then the corresponding competing protein was titrated to the reaction mixture at varying concentrations. After 3 hr of equilibration, the reaction mixture was run on a 5% native polyacrylamide gel in 1× Tris-borate (TB) for 3 hr at 120 V. Quantifications were done by determining the pixel intensity of the RNA species bound by protein relative to the pixel intensity of total RNA species to give the fraction bound of RNA. The pixel intensities of each band were determined and background-corrected by using Image Gauge (Fujifilm).

NEG-1::GFP Quantification

Time-lapse imaging of NEG-1::GFP was conducted by capturing GFP fluorescence (exposure time, 40 ms) at three different planes (z stacks) every 1 min from the two- to six-cell stages. Images spanning the four-cell stage were analyzed by measuring GFP intensity in nuclei (mean gray value) using ImageJ. The three time points preceding the division of ABa and ABp were selected to represent NEG-1::GFP intensity in the four-cell stage. GFP intensity of ABa and ABp were summed for "anterior GFP," and those of EMS and P2 were summed for "posterior GFP" (NEG-1::GFP asymmetry = anterior GFP – posterior GFP).

Embryonic Cell Lineaging and *pha-4::gfp* Expression

The EMS lineage was performed using the *pha-4::gfp* lineaging strain RW10425 for the wild-type. The strain was fed *pos-1* RNAi food to lineage EMS in *pos-1(–)* embryos. The strain was crossed with *pos-1(zu148) unc-42(e270)* and fed *gld-3* RNAi food to lineage EMS in *pos-1(–); gld-3(–)* embryos. Lineaging was performed according to Du et al. (2014). The images of *pha-4::gfp* expression generated during lineaging were used for Figure 6C.

PAT-Seq

The PAT-seq approach was utilized to determine the gene expression, poly(A) site, and polyadenylation state of the transcriptome of early *C. elegans* embryos having been depleted for a series of RNA binding proteins. *pos-1* was knocked down using double-stranded RNA (dsRNA)-expressed *E. coli* fed to ~100,000 starved/synchronized L1 larvae. When half of the population reached adulthood and half were still in the L4 stage, worms were bleached and embryos harvested and stored in Trizol. This ensured an enrichment of early embryos between the 1- and 24-cell stage. Because prolonged *gld-3* and *gld-2* RNAi causes sterility, starved/synchronized L1 larvae were fed diluted OP50 (200 μl of concentrated OP50 diluted in 2 ml of M9 and starved L1s) for 16 hr. After this initial step, the OP50 was mostly consumed by the larvae, and concentrated *gld-3* or *gld-2* dsRNA expressing *E. coli* was added to the plates. When half of the population reached adulthood and half were still in the L4 stage, worms were bleached and embryos harvested and stored in

Trizol. Total RNA was isolated using standard procedures. For wild-type samples, synchronized L1s were fed OP50 until the aforementioned stage before being processed as stated above. More than 90% knockdown of *pos-1* and *gld-3* was confirmed by qPCR, whereas the *gld-2* knockdown was approximately 50% (data not shown).

Osmotic Avoidance Test

A drop of glycerol (2 M) was delivered near the tail of a worm as it moved forward. The glycerol drop instantly surrounds the worm and reaches the anterior sensory organs. Wild-type worms immediately sense the glycerol as a repellent and move backward. Backward movement was scored.

ACCESSION NUMBERS

The GEO accession number for the PAT-seq data reported in this paper is GSE57993.

SUPPLEMENTAL INFORMATION

Supplemental Information includes five figures, three tables, and two movies and can be found with this article online at http://dx.doi.org/10.1016/j.devcel.2015.05.024.

AUTHOR CONTRIBUTIONS

A.E. and C.C.M designed the experiments and wrote the paper. A.E., M.S., H.W., and D.Y. developed the transgenic worms. M.S. performed the *med-1* in situ hybridization. A.E., E.K., and S.R. performed, analyzed, and interpreted the in vitro gel shift assays. A.E., P.F.H., D.R.P., and T.H.B. performed, analyzed, and interpreted the PAT-seq experiments. A.E., Z.D., and Z.B. performed the cell lineaging study. A.E., C.D.C., and J.S. performed, analyzed, and interpreted the behavior assay. T.I. performed additional imaging trials to quantify NEG-1::GFP intensity.

ACKNOWLEDGMENTS

We thank the Mello and Ambros labs for input and discussion, Darryl Conte and Myriam Aouadi for comments on the text and figures, and James Mello for critical reading of the manuscript. *neg-1(tm6077)* was generated by Shohei Mitani. This work was supported by NIH grants HD36247 and HD33769 (to C.C.M.). C.C.M is a Howard Hughes Medical Institute Investigator.

Received: December 19, 2014
Revised: April 17, 2015
Accepted: May 27, 2015
Published: June 18, 2015

REFERENCES

Barnard, D.C., Ryan, K., Manley, J.L., and Richter, J.D. (2004). Symplekin and xGLD-2 are required for CPEB-mediated cytoplasmic polyadenylation. Cell *119*, 641–651.

Begasse, M.L., and Hyman, A.A. (2011). The first cell cycle of the Caenorhabditis elegans embryo: spatial and temporal control of an asymmetric cell division. Results Probl. Cell Differ. *53*, 109–133.

Benoit, P., Papin, C., Kwak, J.E., Wickens, M., and Simonelig, M. (2008). PAP- and GLD-2-type poly(A) polymerases are required sequentially in cytoplasmic polyadenylation and oogenesis in Drosophila. Development *135*, 1969–1979.

Bowerman, B., Eaton, B.A., and Priess, J.R. (1992). skn-1, a maternally expressed gene required to specify the fate of ventral blastomeres in the early C. elegans embryo. Cell *68*, 1061–1075.

Chicoine, J., Benoit, P., Gamberi, C., Paliouras, M., Simonelig, M., and Lasko, P. (2007). Bicaudal-C recruits CCR4-NOT deadenylase to target mRNAs and regulates oogenesis, cytoskeletal organization, and its own expression. Dev. Cell *13*, 691–704.

Crittenden, S.L., Eckmann, C.R., Wang, L., Bernstein, D.S., Wickens, M., and Kimble, J. (2003). Regulation of the mitosis/meiosis decision in the Caenorhabditis elegans germline. Philos. Trans. R. Soc. Lond. B Biol. Sci. *358*, 1359–1362.

Cui, J., Sackton, K.L., Horner, V.L., Kumar, K.E., and Wolfner, M.F. (2008). Wispy, the Drosophila homolog of GLD-2, is required during oogenesis and egg activation. Genetics *178*, 2017–2029.

D'Ambrogio, A., Nagaoka, K., and Richter, J.D. (2013). Translational control of cell growth and malignancy by the CPEBs. Nat. Rev. Cancer *13*, 283–290.

Darnell, J.C., and Richter, J.D. (2012). Cytoplasmic RNA-binding proteins and the control of complex brain function. Cold Spring Harb. Perspect. Biol. *4*, a012344.

DeRenzo, C., Reese, K.J., and Seydoux, G. (2003). Exclusion of germ plasm proteins from somatic lineages by cullin-dependent degradation. Nature *424*, 685–689.

Draper, B.W., Mello, C.C., Bowerman, B., Hardin, J., and Priess, J.R. (1996). MEX-3 is a KH domain protein that regulates blastomere identity in early C. elegans embryos. Cell *87*, 205–216.

Du, Z., Santella, A., He, F., Tiongson, M., and Bao, Z. (2014). De novo inference of systems-level mechanistic models of development from live-imaging-based phenotype analysis. Cell *156*, 359–372.

Eckmann, C.R., Crittenden, S.L., Suh, N., and Kimble, J. (2004). GLD-3 and control of the mitosis/meiosis decision in the germline of Caenorhabditis elegans. Genetics *168*, 147–160.

Eckmann, C.R., Rammelt, C., and Wahle, E. (2011). Control of poly(A) tail length. Wiley Interdiscip. Rev. RNA *2*, 348–361.

Farley, B.M., Pagano, J.M., and Ryder, S.P. (2008). RNA target specificity of the embryonic cell fate determinant POS-1. RNA *14*, 2685–2697.

Frøkjaer-Jensen, C., Davis, M.W., Hopkins, C.E., Newman, B.J., Thummel, J.M., Olesen, S.P., Grunnet, M., and Jorgensen, E.M. (2008). Single-copy insertion of transgenes in Caenorhabditis elegans. Nat. Genet. *40*, 1375–1383.

Goldstein, B. (1992). Induction of gut in Caenorhabditis elegans embryos. Nature *357*, 255–257.

Guven-Ozkan, T., Nishi, Y., Robertson, S.M., and Lin, R. (2008). Global transcriptional repression in C. elegans germline precursors by regulated sequestration of TAF-4. Cell *135*, 149–160.

Hardin, J. (2011). Imaging embryonic morphogenesis in C. elegans. Methods Cell Biol. *106*, 377–412.

Horner, M.A., Quintin, S., Domeier, M.E., Kimble, J., Labouesse, M., and Mango, S.E. (1998). pha-4, an HNF-3 homolog, specifies pharyngeal organ identity in Caenorhabditis elegans. Genes Dev. *12*, 1947–1952.

Hwang, S.Y., and Rose, L.S. (2010). Control of asymmetric cell division in early C. elegans embryogenesis: teaming-up translational repression and protein degradation. BMB Rep. *43*, 69–78.

Ivshina, M., Lasko, P., and Richter, J.D. (2014). Cytoplasmic polyadenylation element binding proteins in development, health, and disease. Annu. Rev. Cell Dev. Biol. *30*, 393–415.

Jänicke, A., Vancuylenberg, J., Boag, P.R., Traven, A., and Beilharz, T.H. (2012). ePAT: a simple method to tag adenylated RNA to measure poly(A)-tail length and other 3′ RACE applications. RNA *18*, 1289–1295.

Kim, K.W., Wilson, T.L., and Kimble, J. (2010). GLD-2/RNP-8 cytoplasmic poly(A) polymerase is a broad-spectrum regulator of the oogenesis program. Proc. Natl. Acad. Sci. USA *107*, 17445–17450.

Kwak, J.E., Wang, L., Ballantyne, S., Kimble, J., and Wickens, M. (2004). Mammalian GLD-2 homologs are poly(A) polymerases. Proc. Natl. Acad. Sci. USA *101*, 4407–4412.

Maduro, M.F., Meneghini, M.D., Bowerman, B., Broitman-Maduro, G., and Rothman, J.H. (2001). Restriction of mesendoderm to a single blastomere by the combined action of SKN-1 and a GSK-3beta homolog is mediated by MED-1 and -2 in C. elegans. Mol. Cell *7*, 475–485.

Maduro, M.F., Broitman-Maduro, G., Mengarelli, I., and Rothman, J.H. (2007). Maternal deployment of the embryonic SKN-1—>MED-1,2 cell specification pathway in C. elegans. Dev. Biol. *301*, 590–601.

Mangus, D.A., Evans, M.C., and Jacobson, A. (2003). Poly(A)-binding proteins: multifunctional scaffolds for the post-transcriptional control of gene expression. Genome Biol. *4*, 223.

McMahon, L., Legouis, R., Vonesch, J.L., and Labouesse, M. (2001). Assembly of C. elegans apical junctions involves positioning and compaction by LET-413 and protein aggregation by the MAGUK protein DLG-1. J. Cell Sci. *114*, 2265–2277.

Mello, C.C., Draper, B.W., Krause, M., Weintraub, H., and Priess, J.R. (1992). The pie-1 and mex-1 genes and maternal control of blastomere identity in early C. elegans embryos. Cell *70*, 163–176.

Mello, C.C., Draper, B.W., and Priess, J.R. (1994). The maternal genes apx-1 and glp-1 and establishment of dorsal-ventral polarity in the early C. elegans embryo. Cell *77*, 95–106.

Mello, C.C., Schubert, C., Draper, B., Zhang, W., Lobel, R., and Priess, J.R. (1996). The PIE-1 protein and germline specification in C. elegans embryos. Nature *382*, 710–712.

Nakanishi, T., Kubota, H., Ishibashi, N., Kumagai, S., Watanabe, H., Yamashita, M., Kashiwabara, S., Miyado, K., and Baba, T. (2006). Possible role of mouse poly(A) polymerase mGLD-2 during oocyte maturation. Dev. Biol. *289*, 115–126.

Nakel, K., Hartung, S.A., Bonneau, F., Eckmann, C.R., and Conti, E. (2010). Four KH domains of the C. elegans Bicaudal-C ortholog GLD-3 form a globular structural platform. RNA *16*, 2058–2067.

Ogura, K., Kishimoto, N., Mitani, S., Gengyo-Ando, K., and Kohara, Y. (2003). Translational control of maternal glp-1 mRNA by POS-1 and its interacting protein SPN-4 in Caenorhabditis elegans. Development *130*, 2495–2503.

Osborne Nishimura, E., Zhang, J.C., Werts, A.D., Goldstein, B., and Lieb, J.D. (2015). Asymmetric transcript discovery by RNA-seq in C. elegans blastomeres identifies neg-1, a gene important for anterior morphogenesis. PLoS Genet. *11*, e1005117.

Pagano, J.M., Farley, B.M., McCoig, L.M., and Ryder, S.P. (2007). Molecular basis of RNA recognition by the embryonic polarity determinant MEX-5. J. Biol. Chem. *282*, 8883–8894.

Pagano, J.M., Farley, B.M., Essien, K.I., and Ryder, S.P. (2009). RNA recognition by the embryonic cell fate determinant and germline totipotency factor MEX-3. Proc. Natl. Acad. Sci. USA *106*, 20252–20257.

Priess, J.R., and Thomson, J.N. (1987). Cellular interactions in early C. elegans embryos. Cell *48*, 241–250.

Richter, J.D., and Lasko, P. (2011). Translational control in oocyte development. Cold Spring Harb. Perspect. Biol. *3*, a002758.

Schubert, C.M., Lin, R., de Vries, C.J., Plasterk, R.H., and Priess, J.R. (2000). MEX-5 and MEX-6 function to establish soma/germline asymmetry in early C. elegans embryos. Mol. Cell *5*, 671–682.

Seydoux, G., and Dunn, M.A. (1997). Transcriptionally repressed germ cells lack a subpopulation of phosphorylated RNA polymerase II in early embryos of Caenorhabditis elegans and Drosophila melanogaster. Development *124*, 2191–2201.

Tabara, H., Hill, R.J., Mello, C.C., Priess, J.R., and Kohara, Y. (1999). pos-1 encodes a cytoplasmic zinc-finger protein essential for germline specification in C. elegans. Development *126*, 1–11.

Tenlen, J.R., Schisa, J.A., Diede, S.J., and Page, B.D. (2006). Reduced dosage of pos-1 suppresses Mex mutants and reveals complex interactions among CCCH zinc-finger proteins during Caenorhabditis elegans embryogenesis. Genetics *174*, 1933–1945.

Wang, L., Eckmann, C.R., Kadyk, L.C., Wickens, M., and Kimble, J. (2002). A regulatory cytoplasmic poly(A) polymerase in Caenorhabditis elegans. Nature *419*, 312–316.

Weill, L., Belloc, E., Bava, F.A., and Méndez, R. (2012). Translational control by changes in poly(A) tail length: recycling mRNAs. Nat. Struct. Mol. Biol. *19*, 577–585.

Zhang, Y., Park, S., Blaser, S., and Sheets, M.D. (2014). Determinants of RNA binding and translational repression by the Bicaudal-C regulatory protein. J. Biol. Chem. *289*, 7497–7504.